Antarctic vortex dehydration in 2023 as a substantial removal pathway for Hunga Tonga-Hunga Ha'apai water vapour

Xin Zhou[1,2], Sandip S. Dhomse[2,3], Wuhu Feng[2,4], Graham Mann[2], Saffron Heddell[2], Hugh Pumphrey[5], Brian J. Kerridge[6], Barry Latter[6], Richard Siddans[6], Lucy Ventress[6], Richard Querel[7], Penny Smale[7], Elizabeth Asher[8,9], Emrys G. Hall[9], Slimane Bekki[10], Martyn P. Chipperfield[2,3]

[1]School of Atmospheric Sciences, Chengdu University of Information Technology, Chengdu, China
[2]School of Earth and Environment, University of Leeds, Leeds, UK
[3]National Centre for Earth Observation, University of Leeds, Leeds, UK
[4]National Centre for Atmospheric Science, University of Leeds, Leeds, UK
[5]School of GeoSciences, The University of Edinburgh, Edinburgh, UK
[6]NCEO, STFC Rutherford Appleton Laboratory, Oxon, UK
[7]National Institute of Water and Atmospheric Research (NIWA), Lauder, New Zealand
[8]Cooperative Institute for Research in Environmental Sciences, University of Colorado, Boulder, CO, USA
[9]NOAA Global Monitoring Laboratory, Boulder, CO, USA
[10]LATMOS/IPSL, Sorbonne Université, UVSQ, CNRS, Paris, France

Key Points:

- Antarctic dehydration is a major removal pathway of stratospheric H_2O injected from Hunga Tonga-Hunga Ha'apai (HTHH) eruption
- HTHH H_2O caused small (up to 10 DU) additional chemical ozone depletion in 2023 Antarctic spring
- Model indicates e-folding timescale of 4 years for removal of HTHH H_2O from stratosphere

Corresponding author: Xin Zhou, x.zhou1@leeds.ac.uk

Abstract

The January 2022 eruption of Hunga Tonga-Hunga Ha'apai (HTHH) injected a huge amount (∼150 Tg) of water vapour (H_2O) into the stratosphere, along with small amount of SO_2. An off-line 3-D chemical transport model (CTM) successfully reproduces the spread of the injected H_2O through October 2023 as observed by the Microwave Limb Sounder (MLS). Dehydration in the 2023 Antarctic polar vortex caused the first substantial (∼20 Tg) removal of HTHH H_2O from the stratosphere. The CTM indicates that this process will dominate removal of HTHH H_2O for the coming years, giving an overall e-folding timescale of 4 years; around 25 Tg of the injected H_2O is predicted to still remain in the stratosphere by 2030. Following relatively low Antarctic column ozone in midwinter 2023 due to transport effects, additional springtime depletion due to H_2O-related chemistry was small and maximised at the vortex edge (10 DU in column).

Plain Language Summary

Around 150 Tg (150 million tons) of water vapour was injected into the stratosphere during the eruption of Hunga Tonga-Hunga Ha'apai. Water vapour is a greenhouse gas and this increase is expected to have a warming effect in the troposphere, as well causing perturbations in stratospheric chemistry and aerosols. We use an atmospheric model to study the residence time of this excess water vapour and its impact on the recent Antarctic ozone hole. The model performance is evaluated by comparison with satellite measurements. Wintertime dehydration in the Antarctic stratosphere in 2023 is found to be an important mechanism for removal of the volcanic water from the stratosphere. However, the overall removal rate is predicted to be slow; around 25 Tg (17%) is still present in 2030. The direct impact of the excess water vapour on ozone via chemical processes in the Antarctic ozone hole in 2023 is small.

1 Introduction

The eruption on 15^{th} January 2022 of the submarine Hunga Tonga - Hunga Ha'apai (HTHH) volcano (20.54°S, 175.38°W) is recognized as the most explosive in the last 30 years, with emissions reaching up to ∼55 km (Carr et al., 2022; Taha et al., 2022). It was unusual due to the huge amount of water vapour (H_2O) injected very high into the stratosphere, along with only small quantities of sulfur dioxide (SO_2), thereby challenging many preconceptions about the atmospheric impacts of volcanic eruptions. This exceptional event is a global experiment allowing us to study, for the first time, a water-rich volcanic eruption. Microwave Limb Sounder (MLS) satellite measurements indicate that around 150 Tg of H_2O was injected, increasing the stratospheric burden by around 10% (Millán et al., 2022; Xu et al., 2022; Khaykin et al., 2022), while the SO_2 injection was only 0.5 Tg. This is expected to generate a very different climate forcing to other satellite-observed SO_2-rich volcanic eruptions, possibly leading to a net warming of the global surface temperature due to the dominant radiative effect of H_2O perturbations (Sellitto et al., 2022; Jenkins et al., 2023).

The slow spreading of the injected H_2O throughout the stratosphere via the Brewer-Dobson circulation (BDC) (Coy et al., 2022; Manney et al., 2023) is also expected to affect stratospheric chemistry and dynamics. Rapid ozone depletion was observed in the initial plume (Evan et al., 2023), along with the rapid formation of a dense aerosol layer as a result of the water vapour injection (Asher et al., 2023; Zhu et al., 2022). In addition, evident processing of chlorine and depletion of nitrogen was observed in the southern tropical stratosphere immediately after the HTHH eruption, which then spread poleward over the following months (Santee et al., 2023). The aerosol layer was transported polewards at lower altitudes than the H_2O enhancement. The excess H_2O caused a strong cooling in the SH mid-latitude stratosphere shortly after the eruption (Schoeberl et al., 2022; Vömel et al., 2022), which in turn strengthened the mid-latitude jet and slowed down the BDC (Coy et al., 2022). When the HTHH H_2O reaches high latitudes with the descent of the BDC, it can affect gas-phase and heterogeneous processes related to polar ozone loss. Determining the timing and longevity of the excess H_2O is thus critically important for assessing the impact on stratospheric ozone recovery and near-term climate change.

Water vapour can affect processes that drive stratospheric ozone in many ways. One important example is the formation of polar stratospheric clouds (PSCs), which initiate ozone-depleting heterogeneous chemistry. Sedimentation of ice PSCs irreversibly changes the H_2O amount in the polar vortex, and affects the ozone-depletion processes via dehydration and denitrification (e.g., Fahey et al., 2001; Kelly et al., 1989; Feng et al., 2011; Tabazadeh et al., 2000). Dehydration in Antarctic winter has long been observed (e.g., Kelly et al., 1989; Vömel et al., 1995; Rosenlof et al., 1997; Tomikawa et al., 2015), but its representation by models can vary when applying PSC schemes with different complexity. If we use the HTHH water transport and its dehydration at polar regions as metrics to test a model's stratospheric transport and PSC processes, we can then predict the longevity of the excess H_2O by calculating its annual removal amount.

In this paper we use an off-line 3-D chemical transport model (CTM) to simulate the spatio-temporal evolution of the injected H_2O with the results showing good agreement with MLS measuremensts in terms of plume spread and removal of HTHH H_2O from the stratosphere. We estimate the longevity of the excess H_2O and the amount that may remain in the stratosphere over the coming decade. We also diagnose the direct chemical impact of the increased H_2O on stratospheric ozone through gas-phase and heterogeneous chemistry (e.g. PSCs and aerosols). The impacts are simulated with specified realistic post-eruption meteorology and hence do not account explicitly for dynamical feedbacks. Our CTM setup nonetheless provides useful constraints on changes seen in more complex coupled radiative-dynamical-chemical models (Wang et al., 2023).

2 Model and Observations

The TOMCAT/SLIMCAT CTM (Chipperfield, 1999, 2006) was run at a horizontal resolution of 2.8°×2.8° and 32 levels from the surface to about 60 km forced with European Centre for Medium-Range Weather Forecasts (ECMWF) ERA-5 meteorology (Hersbach et al., 2020). The model uses a detailed gas-phase stratospheric chemistry scheme, and a simplified PSC scheme for the simulation of heterogeneous chemistry based on the assumption of thermodynamic equilibrium between PSC particles, including liquid aerosol, solid nitric acid trihydrate, and/or solid ice particles (Grooß et al., 2018), and the gas phase (e.g., Feng et al., 2011, 2021). In this scheme, ice particles with assumed radius of 10 μm sediment with a fall velocity of 1500 m/day. A control simulation (**Control**) without treatment of HTHH was integrated from 1980 to October 2023. Output from run **Control** for January 1st 2022 was used to intialise a run (**HT**) until October 31st 2023 with the injection of 150 Tg of H_2O into the low-mid stratosphere at southern subtropical latitudes. We experimented with the timing of the model H_2O injection between January 15th and April 1st. A later injection date, when the plume is already well spread longitudinally and latitudinally (i.e. April 1st, 0°-360°E, 2°S-28°S), overcomes inconsistencies between the initial plume dynamics and the coarse resolution CTM. The model used here employs a climatological distribution of H_2O in the troposphere, so that any excess H_2O transported to this region is removed from the model. The runs used background fields for sulfuric acid aerosols with no enhancement due to HTHH. The magnitude and impact of the HTHH SO_2 is uncertain (Wang et al., 2023) and in this study we focus on H_2O alone.

To test the possible future evolution of the HTHH H_2O three further model runs were performed. These were integrated from January 1st 2023 until 2030 using repeating ERA-5 meteorology for 2022. Run **Con_2022** was essentially an extension of run **Control**; run **HT_2022** was an extension of **HT**; run **HT_2022ns** was the same as run **HT_2022** but had sedimentation of PSC particles turned off. The experiments are summarized in Supplementary Table S1.

The modelled results are compared to satellite measurements of H_2O from MLS (Waters et al., 2006) and total column ozone from the Ozone Monitoring Instrument (OMI) (Levelt et al., 2006) on the NASA Aura satellite, and the Infrared Atmospheric Sounding Interferometer (IASI) (Siddans et al., 2018) on MetOp-B satellite.

MLS H_2O anomalies are calculated as deviations from the climatology of 2005-2021. The stratospheric total mass of H_2O is estimated as the global (80°S-80°N) sum of the stratospheric column over each 5° latitude band from MLS volume mixing ratio measurements on pressure levels. For this study, we use MLS version 4 (v4) and version 5 (v5) products for the H_2O mass, but use v4 for analysis of the vertical structure of the plume in view of the poor fits of v5 to H_2O signals in regions with extremely enhanced humidity (Millán et al., 2022).

3 Evaluation of the model post-eruption stratospheric transport

We first assess the model performance for the H_2O transport after eruption. Figure 1a shows the H_2O anomaly profiles after the HTHH injection in model run **HT** (dashed line), compared with MLS measurements (solid line). The two are in good agreement, both showing the positive water vapour anomaly of 8–11 ppmv peaking between 30 hPa and 10 hPa from April to September. While the injected total mass in the model is consistent with MLS, the simulation has slightly larger peak anomalies and smaller horizontal extent after injection. The simulated plume spread is in very good agreement with the observations (Figure 1b and Supplementary Movie S1), in particular regarding the characteristics and behaviour of the excess H_2O at the mixing barriers in the stratosphere, including the polar vortex edge, the extratropical tropopause, and the tropical pipe. Around 4-6 months after the eruption, the excess H_2O moves into the Southern Hemisphere (SH) mid-latitudes within the shallow branch of the BDC, i.e. via the tropical pipe (Plumb, 1996). However, it does not intrude into the 2022 Antarctic polar vortex due to the polar jet. Only after the breakdown of the Antarctic polar vortex in November 2022 did the H_2O reach the pole (see also Manney et al. (2023)). The circulation associated with the easterly phase of the Quasi-Biennial Oscillation (QBO) confine the excess H_2O to the SH until the transition to westerlies at the end of 2022. When the SH moves into austral winter, H_2O enters the deep branch of the BDC, ascending from the tropics and descending into the high latitudes in the SH. The model reproduces well the timing of the HTHH-injected H_2O penetrating the polar vortex, and the altitudes of the H_2O plume. This indicates the model has a good representation of both the poleward horizontal H_2O transport by the shallow branch of the BDC and the ascent of the water-enriched air to high levels by the deep branch of the BDC.

4 Dehydration in 2023 Antarctic winter

Figure 2a shows the time evolution series of total excess stratospheric H_2O mass above 68 hPa observed by the MLS. After the enhancement of the stratospheric H_2O mass by $\sim$150 Tg after HTHH injection in January 2022, the amount of excess H_2O remained steady until a sudden drop of $\sim$20 Tg from June to July 2023. This strong dehydration is also seen in the time series of the Antarctic H_2O mixing ratio at 31 hPa (Figure 2b). First, the excess H_2O rose to its highest and unprecedented level at the end of May 2023 in this 20-year record, when the HTHH injected H_2O entered the Antarctic stratosphere via the deep branch of the BDC. Then, a striking drop in H_2O occurred within just three months from June to August 2023. The H_2O anomaly fell from 2.5 ppmv to close to zero in August 2023. The amplitude of this stratospheric dehydration is also unprecedented

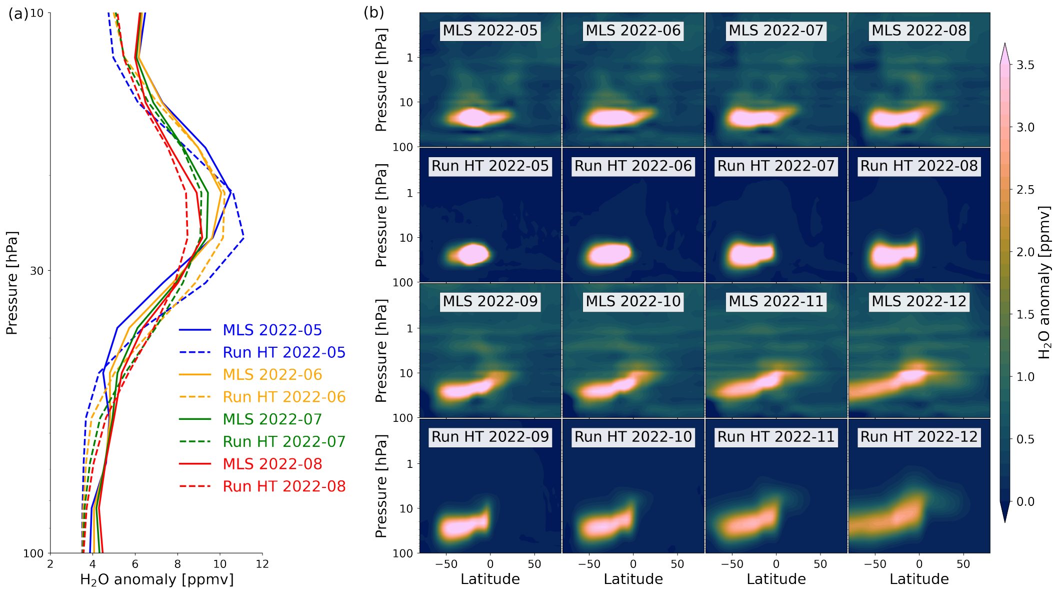

Figure 1. Water vapour (H_2O) profile and evolutions after the HTHH eruption. (a) Zonal mean H_2O anomaly profiles (ppmv) between 40°S-20°S from May to September 2022 from MLS v4 observations (solid lines) and run **HT** (dashed lines). (b) Zonal mean latitude-pressure cross sections of H_2O anomalies observed by MLS v4 and simulated by model run **HT** from May to December 2022.

in the observational record since 2004. The fact that the H_2O anomaly returns to essentially zero in August, like the previous years, shows that the vortex H_2O is controlled by the local polar temperatures (so that water vapour remaining in the gas-phase is determined by its saturation vapour pressure) and is not affected by additional volcanic injection; i.e. ice PSC processes effectively cancel out the in-vortex impact of the additional HTHH water vapour by the end of Austral winter. Note that the model has a good representation of H_2O inside the Antarctic polar vortex core in winter/spring 2023 (Figure S1).

Figures 2c and 2d show the daily tendencies of the H_2O mixing ratio inside the Antarctic vortex observed by MLS v4 and simulated by the model. The dramatic dehydrated areas above 68 hPa are clearly seen in the lower stratosphere in June 2023 with the largest rate of H_2O decrease of -0.19 ppmv/day. This led to a fast transition of the lower stratosphere from anomalously wet conditions to dry in the Antarctic vortex core. The region of strong dehydration is in good agreement with the vertical domain of PSCs that are usually observed between 15 and 25 km. The strong dehydration is accompanied by an increase in H_2O mixing ratio below, indicating enriched H_2O below the dehydrated region. This dehydration and rehydration below are visible until August. Importantly, we see a clear descent of the rehydration over time, causing water originating from higher altitudes to accumulate initially in the polar lowermost stratosphere. The dehydrated and rehydrated air carries on descending throughout winter forced by the BDC with ultimately H_2O being irreversibly removed from the stratosphere. Based on the good agreement between the model simulation and MLS data, the observed dehydration and rehydration below can only be linked to the sedimentation of the ice PSC particles, evaporation at lower levels and descent of this rehydrated air with the BDC. The important consequence is that a substantial amount of HTHH H_2O is removed from the stratosphere during the austral winter.

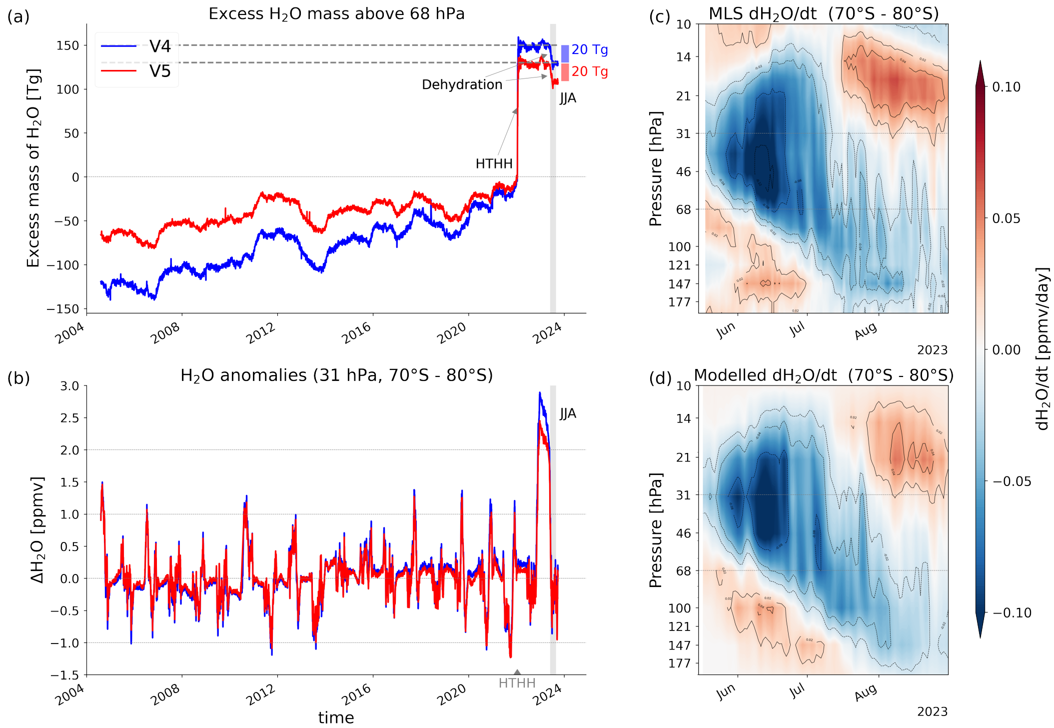

Figure 2. MLS observed and TOMCAT simulated dehydration of the Antarctic polar vortex. (a) Time series of observed excess H_2O mass (Tg) above 68 hPa from MLS v4 and v5. (b) As panel (a) but for MLS v4 mean SH polar cap (80°S-70°S) H_2O mixing ratio (ppmv) at 31 hPa. The grey bar marks the months of June, July and August 2023. (c) MLS v4 observed daily tendencies of mean SH polar cap H_2O mixing ratio (ppmv/day) with a 30-day smoothing from June to August in 2023. (d) Same as (c) but for TOMCAT simulated (run **HT**) daily tendencies.

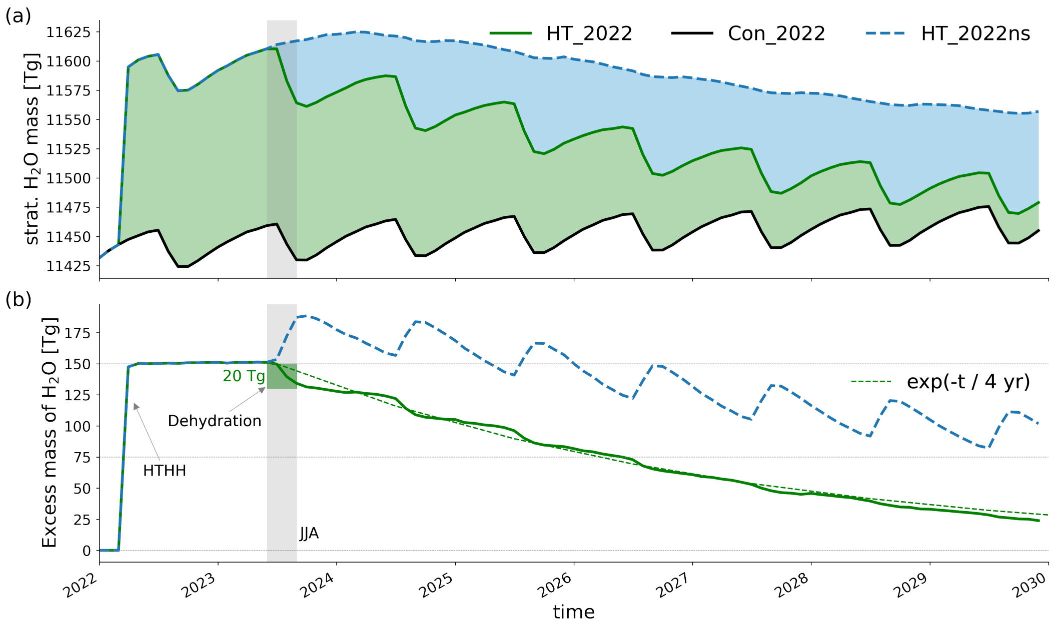

Figure 3. TOMCAT projections of the decay rate of the excess H_2O. (a) Time series of simulated total abundance of H_2O above 100 hPa (Tg) for runs **Con_2022**, **HT_2022**, and **HT_2022ns**. Grey shading indicates the Austral winter (JJA) 2023. (b) Differences (Tg) in panel (a) with respect to control run **Con_2022** for runs **HT_2022** and **HT_2022ns**. The dotted curve illustrates exponential decay with timescale of 4 years starting in July 2023. A horizontal dotted line indicates 75 Tg, 50% of the initial injection.

5 Long-term decay of HTHH water vapour

To clarify the mechanism for the removal of the HTHH injected H_2O, we compare simulations **HT_2022**, **HT_2022ns** and **Con_2022**. Figure 3a shows the total burden of gas phase H_2O above 100 hPa projected by TOMCAT simulation through 2030 for these runs. The annual cycle for run **Con_2022**, with a decrease in austral winter and increase afterward, is related to the annual cycle of its sinks and sources, the dehydration inside the polar vortex in June to August, and the tape recorder signal with enhanced H_2O from the tropical troposphere to the stratosphere that has maximum enhancement around September. A similar annual cycle exists in run **HT_2022**. The differences between the two runs is because the dehydration is stronger for run **HT_2022**, causing a decreasing year-to-year difference between them. In contrast, the run **HT_2022ns** does not show this strong dehydration and annual cycle, with a slower decay throughout the following years. Here, the H_2O decay is caused by the stratosphere-to-troposphere transport where stratospheric air with HTHH-injected H_2O slowly descends into the troposphere at high latitudes via the deep branch of the BDC and is replaced by air from the troposphere with H_2O values determined by tropopause temperatures.

Figure 3b shows the differences in the total burden of H_2O mass between the HTHH perturbed runs and the control run. The excess H_2O, once injected into the stratosphere, is removed in an almost step-like fashion during austral winter starting in 2023. The amount of H_2O removal, around 20 Tg in 2023, is in very good agreement with the MLS observed value, supporting the TOMCAT representation of the HTHH H_2O transport and removal. The modelled e-folding lifetime for the removal of the excess H_2O is around 4 years (half-life of $\sim$2.8 yrs) from the point at which removal starts (over a year after the eruption),

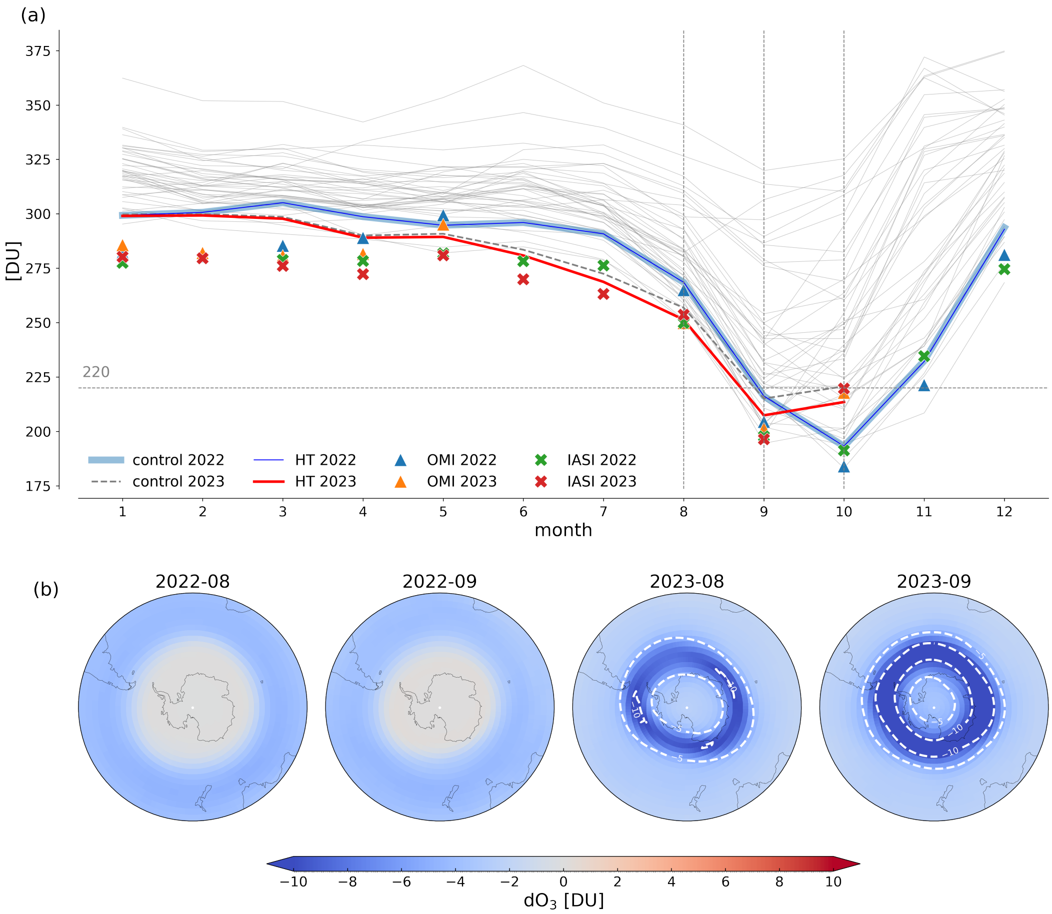

Figure 4. Stratospheric ozone changes after HTHH. (a) Time series of the mean total column ozone (DU) at SH high-latitudes (65°S-90°S), comparing run **Control** in 2022 (bold blue), 2023 (dashed grey) and years 1980 to 2021 (grey) with run **HT** in 2022 (thin navy) and 2023 (solid red), and with OMI (triangle), and IASI (cross) satellite observations in 2022 and 2023. (b) Modelled monthly mean difference in column ozone (DU) between runs **HT** and **Control** for August and September in 2022 and 2023.

so that ~25 Tg remains in the stratosphere at 2030. The longevity of the HTHH injected H_2O thus exceeds 7 years. Comparing the simulated H_2O mass in the stratosphere between runs **HT_2022** and **HT_2022ns**, it can be seen that PSC sedimentation plays a key role in the removal of the HTHH H_2O. Without PSC sedimentation, the decline of H_2O mass is much slower so that only around 50 Tg H_2O is removed by 2030, accounting for ~38% of the total removal in run **HT_2022** by that time. The dehydration due to the sedimentation of ice PSC particles thus accounts for more than 60% of the modelled total removal over this period, serving as a main removal pathway of the HTHH H_2O. It is worth noting that PSC sedimentation is also important for the removal of background (non-volcanic) H_2O. Without PSC sedimentation (run **HT_2022ns**) the stratospheric total H_2O burden would increase slightly during austral winter under the effect of the positive anomalies in H_2O at the tropical tropopause (Gilford & Solomon, 2017). In the model PSC sedimentation removes ~30 Tg of background H_2O each austral winter.

6 Ozone depletion due to the increased H_2O

We now quantify the impact of the additional H_2O on Antarctic ozone through October 2023 and compare with previous years (Figure 4). In 2022, there is negligible modelled chemical impact on the total column ozone at high SH latitudes (65°S-90°S), consistent with the failure of HTHH H_2O to penetrate into the Antarctic polar vortex. In contrast, in 2023 it reached the pole before the vortex formation and thus caused a direct impact. Interestingly, in mid-winter 2023, before the onset of substantial chemical ozone depletion, modelled column ozone is smaller than other modelled years since 1980. This apparent earlier start of the ozone hole was observed by IASI. However, the small difference (10 DU) between model runs **HT** and **Control** shows that this early onset was dynamically driven rather than a chemical impact of the enhanced H_2O. The HTHH injection has been found to be linked to a stable and colder-than-normal vortex, with a slowdown of the BDC (Wang et al., 2023); our CTM may be capturing this effect via the specified ERA-5 meteorology but here we cannot quantify it. An unusual transport of ozone-poor air from the upper stratosphere to the lower stratosphere, indicated by the increase of age-of-air in the stratosphere (Figure S2), can lead to an anomalous decrease of the ozone at lower altitudes.

Meanwhile, an earlier formation of the PSCs can lead to more extensive heterogeneous processing and ozone depletion. However, the strong dehydration due to the sedimentation of ice PSC particles (see above) limits the impact of the additional H_2O in the core of the polar vortex. From June to September, an additional depletion of ozone up to 10 DU (around 4% of the background) due to the injected H_2O occurs at the vortex edge, a region of available sunlight and where ozone loss is not saturated. While the modelled mean column ozone in 2023 is outside the range of previous years in June and July, by September and October it is no longer an outlier. Hence, possible early indications of record low springtime ozone did not occur.

Model runs **Con_2022** and **HT_2022** can be used to estimate the longer term impact of the HTHH H_2O over the next 5 years (Figure S3). The largest column depletion occurs at the edge of the Antarctic vortex in 2023 at 10 DU (see also Figure 4). The impact on the Antarctic ozone hole then decreases in subsequent years as the HTHH H_2O decays. Other large impacts on column ozone occur in the SH midlatitudes in 2022 and, to a lesser extent, the Arctic winter/spring. Interestingly, the impact on the Arctic maximises in winter 2024/25 due to the spread of the HTHH H_2O, but note that these runs use repeating 2022 meteorology. In reality Arctic ozone loss is dominated by meteorological variability.

7 Summary and Discussion

Near-term projections of the HTHH climate impacts depend strongly on the estimation of the transport and longevity of the injected water vapour. Here we show that the Antarctic ice PSC sedimentation is likely a major removal pathway from the stratosphere for the HTHH-injected H_2O. This PSC sedimentation is partly responsible for a small estimated impact on chemical loss in the 2023 Antarctic vortex. Nevertheless, there are many other potential chemical, microphysical and radiative impacts of H_2O (and initial SO_2) in the stratosphere. The projected long residence time of the HTHH H_2O means that we can expect it to influence the atmosphere for many years. Many more modelling and observational studies are needed to quantify these impacts further.

8 Open Research

The v4 MLS water vapour data is available at `https://acdisc.gesdisc.eosdis.nasa.gov/data/Aura_MLS_Level2/ML2H2O.004/`; the v5 data is available at `https://acdisc.gesdisc.eosdis.nasa.gov/data/Aura_MLS_Level2/ML2H2O.005/`. IASI ozone data can be downloaded from the Seris portal `http://iasi.aeris-data.fr/O3/`. OMI total column ozone product is available at `https://disc.gsfc.nasa.gov/datasets/OMDOAO3e_003/summary`. TOMCAT model data is available at `https://doi.org/10.5281/zenodo.10200654` (Zhou, 2023).

Acknowledgments

XZ acknowledges funding from the National Natural Science Foundation of China (42275059; 42175042), China Scholarship Council (201908510032), and Natural Science Foundation of Sichuan Province (2023NSFSC0246; 2022NSFSC1056). MPC and SSD were supported by the NCEO TerraFirma, NERC LSO3 (NE/V011863/1) and ESA OREGANO (4000137112/22/I-AG) projects. WF was supported by the NCAS Long-Term Science programme (NE/R015244/1). SB was supported by the French Agence Nationale de la Recherche (ANR) PyroStrat (Grant: 21-CE01-0028-01) and Centre National d'Etudes Spatiales (CNES) BeSAFE projects. The work at RAL and Leeds was supported by NERC NCEO. The model simulations were performed on the Leeds ARC and UK Archer2 HPC systems. Balloon-borne water vapour measurements were supported by the National Oceanic and Atmospheric Administration (NOAA) Earth Radiation Budget program and by the NOAA Global Monitoring Laboratory. The Antarctic balloon launches at Scott Base were supported by the NZ Government's Strategic Science Investment Fund (SSIF) through the CAAC research programme at NIWA. We thank Antarctica New Zealand (AntNZ) for logistical support.

References

Asher, E., Todt, M., Rosenlof, K., Thornberry, T., Gao, R.-S., Taha, G., ... Xiong, K. (2023). Unexpectedly rapid aerosol formation in the Hunga Tonga plume. *Proceedings of the National Academy of Sciences*, *120*(46), e2219547120. doi: https://doi.org/10.1073/pnas.2219547120

Carr, J. L., Horváth, , Wu, D. L., & Friberg, M. D. (2022). Stereo plume height and motion retrievals for the record-setting Hunga Tonga-Hunga Ha'apai eruption of 15 January 2022. *Geophysical Research Letters*, *49*(9), e2022GL098131. doi: https://doi.org/10.1029/2022GL098131

Chipperfield, M. (1999). Multiannual simulations with a three-dimensional chemical transport model. *Journal of Geophysical Research: Atmospheres*, *104*(D1), 1781–1805. doi: https://doi.org/10.1029/98JD02597

Chipperfield, M. (2006). New version of the TOMCAT/SLIMCAT off-line chemical transport model: Intercomparison of stratospheric tracer experiments. *Quarterly Journal of the Royal Meteorological Society*, *132*(617), 1179–1203. doi: https://doi.org/10.1256/qj.05.51

Coy, L., Newman, P. A., Wargan, K., Partyka, G., Strahan, S. E., & Pawson, S. (2022). Stratospheric circulation changes associated with the Hunga Tonga-Hunga Ha'apai eruption. *Geophysical Research Letters*, *49*(22), e2022GL100982. doi: https://doi.org/10.1029/2022GL100982

Evan, S., Brioude, J., Rosenlof, K. H., Gao, R.-S., Portmann, R. W., Zhu, Y., ... Read, W. G. (2023). Rapid ozone depletion after humidification of the stratosphere by the Hunga Tonga Eruption. *Science*, *382*(6668), eadg2551. doi: https://doi.org/10.1126/science.adg2551

Fahey, D. W., Gao, R. S., Carslaw, K. S., Kettleborough, J., Popp, P. J., Northway, M. J., ... von König, M. (2001). The detection of large HNO_3-containing particles in the winter Arctic stratosphere. *Science*, *291*(5506), 1026-1031. doi: https://doi.org/10.1126/science.1057265

Feng, W., Chipperfield, M. P., Davies, S., Mann, G. W., Carslaw, K. S., Dhomse, S., ... Santee, M. L. (2011). Modelling the effect of denitrification on polar ozone depletion for arctic winter 2004/2005. *Atmospheric Chemistry and Physics*, *11*(13), 6559–6573. doi: https://doi.org/10.5194/acp-11-6559-2011

Feng, W., Dhomse, S. S., Arosio, C., Weber, M., Burrows, J. P., Santee, M. L., & Chipperfield, M. P. (2021). Arctic ozone depletion in 2019/20: Roles of chemistry, dynamics and the Montreal protocol. *Geophysical Research Letters*, *48*(4), e2020GL091911. doi: https://doi.org/10.1029/2020GL091911

Gilford, D. M., & Solomon, S. (2017). Radiative effects of stratospheric seasonal cycles in the tropical upper troposphere and lower stratosphere. *Journal of Climate*, *30*(8), 2769–2783. doi: https://doi.org/10.1175/JCLI-D-16-0633.1

Grooß, J.-U., Müller, R., Spang, R., Tritscher, I., Wegner, T., Chipperfield, M. P., … Madronich, S. (2018). On the discrepancy of HCl processing in the core of the wintertime polar vortices. *Atmospheric Chemistry and Physics*, *18*(12), 8647–8666. doi: https://doi.org/10.5194/acp-18-8647-2018

Hersbach, H., Bell, B., Berrisford, P., Hirahara, S., Horányi, A., Muñoz-Sabater, J., … others (2020). The ERA5 global reanalysis. *Quarterly Journal of the Royal Meteorological Society*, *146*(730), 1999–2049. doi: https://doi.org/10.1002/qj.3803

Jenkins, S., Smith, C., Allen, M., & Grainger, R. (2023). Tonga eruption increases chance of temporary surface temperature anomaly above 1.5° c. *Nature Climate Change*, *13*(2), 127–129. doi: https://doi.org/10.1038/s41558-022-01568-2

Kelly, K. K., Tuck, A. F., Murphy, D. M., Proffitt, M. H., Fahey, D. W., Jones, R. L., … Heidt, L. E. (1989). Dehydration in the lower antarctic stratosphere during late winter and early spring, 1987. *Journal of Geophysical Research: Atmospheres*, *94*(D9), 11317–11357. doi: https://doi.org/10.1029/JD094iD09p11317

Khaykin, S., Podglajen, A., Ploeger, F., Grooß, J.-U., Tencé, F., Bekki, S., … others (2022). Global perturbation of stratospheric water and aerosol burden by Hunga eruption. *Communications Earth & Environment*, *3*(1), 316. doi: https://doi.org/10.1038/s43247-022-00652-x

Levelt, P., van den Oord, G., Dobber, M., Malkki, A., Visser, H., de Vries, J., … Saari, H. (2006). The ozone monitoring instrument. *IEEE Transactions on Geoscience and Remote Sensing*, *44*(5), 1093–1101. doi: https://doi.org/10.1109/TGRS.2006.872333

Manney, G. L., Santee, M. L., Lambert, A., Millán, L. F., Minschwaner, K., Werner, F., … Wang, T. (2023). Siege in the southern stratosphere: Hunga Tonga-Hunga Ha'apai water vapor excluded from the 2022 antarctic polar vortex. *Geophysical Research Letters*, *50*(14), e2023GL103855. doi: https://doi.org/10.1029/2023GL103855

Millán, L., Santee, M. L., Lambert, A., Livesey, N. J., Werner, F., Schwartz, M. J., … Froidevaux, L. (2022). The Hunga Tonga-Hunga Ha'apai hydration of the stratosphere. *Geophysical Research Letters*, *49*, e2022GL099381. doi: https://doi.org/10.1029/2022GL099381

Plumb, R. A. (1996). A "tropical pipe" model of stratospheric transport. *Journal of Geophysical Research: Atmospheres*, *101*(D2), 3957–3972. doi: https://doi.org/10.1029/95JD03002

Rosenlof, K. H., Tuck, A. F., Kelly, K. K., Russell III, J. M., & McCormick, M. P. (1997). Hemispheric asymmetries in water vapor and inferences about transport in the lower stratosphere. *Journal of Geophysical Research: Atmospheres*, *102*(D11), 13213–13234. doi: https://doi.org/10.1029/97JD00873

Santee, M. L., Lambert, A., Froidevaux, L., Manney, G. L., Schwartz, M. J., Millán, L. F., … Fuller, R. A. (2023). Strong evidence of heterogeneous processing on stratospheric sulfate aerosol in the extrapolar Southern Hemisphere following the 2022 Hunga Tonga-Hunga Ha'apai eruption. *Journal of Geophysical Research: Atmospheres*, *128*(16), e2023JD039169. doi: https://doi.org/10.1029/2023JD039169

Schoeberl, M. R., Wang, Y., Ueyama, R., Taha, G., Jensen, E., & Yu, W. (2022).

Analysis and impact of the Hunga Tonga-Hunga Ha'apai stratospheric water vapor plume. *Geophysical Research Letters*, *49*(20), e2022GL100248. doi: https://doi.org/10.1029/2022GL100248

Sellitto, P., Podglajen, A., Belhadji, R., Boichu, M., Carboni, E., Cuesta, J., … others (2022). The unexpected radiative impact of the Hunga Tonga eruption of 15th january 2022. *Communications Earth & Environment*, *3*(1), 288. doi: https://doi.org/10.1038/s43247-022-00618-z

Siddans, R., Walker, J., Latter, B., Kerridge, B., Gerber, D., & Knappett, D. (2018). RAL Infrared Microwave Sounder (IMS) temperature, water vapour, ozone and surface spectral emissivity. centre for environmental data analysis. *Centre for Environmental Data Analysis*. doi: https://dx.doi.org/10.5285/489e9b2a0abd43a491d5afdd0d97c1a4

Tabazadeh, A., Santee, M. L., Danilin, M. Y., Pumphrey, H. C., Newman, P. A., Hamill, P. J., & Mergenthaler, J. L. (2000). Quantifying denitrification and its effect on ozone recovery. *Science*, *288*(5470), 1407-1411. doi: https://doi.org/10.1126/science.288.5470.1407

Taha, G., Loughman, R., Colarco, P. R., Zhu, T., Thomason, L. W., & Jaross, G. (2022). Tracking the 2022 Hunga Tonga-Hunga Ha'apai aerosol cloud in the upper and middle stratosphere using space-based observations. *Geophysical Research Letters*, *49*(19), e2022GL100091. doi: https://doi.org/10.1029/2022GL100091

Tomikawa, Y., Sato, K., Hirasawa, N., Tsutsumi, M., & Nakamura, T. (2015). Balloon-borne observations of lower stratospheric water vapor at Syowa Station, Antarctica in 2013. *Polar Science*, *9*(4), 345–353. doi: https://doi.org/10.1016/j.polar.2015.08.003

Vömel, H., Evan, S., & Tully, M. (2022). Water vapor injection into the stratosphere by Hunga Tonga-Hunga Ha'apai. *Science*, *377*(6613), 1444–1447.

Vömel, H., Oltmans, S., Hofmann, D., Deshler, T., & Rosen, J. (1995). The evolution of the dehydration in the Antarctic stratospheric vortex. *Journal of Geophysical Research: Atmospheres*, *100*(D7), 13919–13926. doi: https://doi.org/10.1029/95JD01000

Wang, X., Randel, W., Zhu, Y., Tilmes, S., Starr, J., Yu, W., … Li, J. (2023). Stratospheric climate anomalies and ozone loss caused by the Hunga Tonga-Hunga Ha'apai volcanic eruption. *Journal of Geophysical Research: Atmospheres*, *128*(22), e2023JD039480. doi: https://doi.org/10.1029/2023JD039480

Waters, J., Froidevaux, L., Harwood, R., Jarnot, R., Pickett, H., Read, W., … Walch, M. (2006). The earth observing system microwave limb sounder (EOS MLS) on the Aura satellite. *IEEE Transactions on Geoscience and Remote Sensing*, *44*(5), 1075–1092. doi: https://doi.org/10.1109/TGRS.2006.873771

Xu, J., Li, D., Bai, Z., Tao, M., & Bian, J. (2022). Large amounts of water vapor were injected into the stratosphere by the Hunga Tonga-Hunga Ha'apai volcano eruption. *Atmosphere*, *13*(6), 912. doi: https://doi.org/10.3390/atmos13060912

Zhou, X. (2023). Datasets used for analysis and plotting in the study by zhou et al. "antarctic vortex dehydration in 2023 as a substantial removal pathway for Hunga Tonga-Hunga Ha'apai water vapour". *Zenodo*. doi: https://doi.org/10.5281/zenodo.10200654

Zhu, Y., Bardeen, C. G., Tilmes, S., Mills, M. J., Wang, X., Harvey, V. L., … others (2022). Perturbations in stratospheric aerosol evolution due to the water-rich plume of the 2022 Hunga-Tonga eruption. *Communications Earth & Environment*, *3*(1), 248. doi: https://doi.org/10.1038/s43247-022-00580-w